Inorg. Chem. **2008**, *47*, 3056−3064

Investigations of Acidity and Nucleophilicity of Diphenyldithiophosphinate Ligands Using Theory and Gas-Phase Dissociation Reactions

Christopher M. Leavitt,[†] Garold L. Gresham,[*,‡] Michael T. Benson,[‡] Jean-Jacques Gaumet,[§] Dean R. Peterman,[‡] John R. Klaehn,[‡] Megan Moser,[‡] Frederic Aubriet,[§] Michael J. Van Stipdonk,[†] and Gary S. Groenewold[‡]

Wichita State University, Wichita, Kansas, Idaho National Laboratory, Idaho Falls, Idaho, and Laboratoire de Spectrometrie de Masse et de Chimie Laser, Université Paul Verlaine–Metz, Metz, France

Received October 22, 2007

Diphenyldithiophosphinate (DTP) ligands modified with electron-withdrawing trifluoromethyl (TFM) substitutents are of high interest because they have demonstrated potential for exceptional separation of Am^{3+} from lanthanide^{3+} cations. Specifically, the *bis*(*ortho*-TFM) (L_1^-) and (*ortho*-TFM)(*meta*-TFM) (L_2^-) derivatives have shown excellent separation selectivity, while the *bis*(*meta*-TFM) (L_3^-) and unmodified DTP (L_u^-) did not. Factors responsible for selective coordination have been investigated using density functional theory (DFT) calculations in concert with competitive dissociation reactions in the gas phase. To evaluate the role of (DTP + H) acidity, density functional calculations were used to predict pK_a values of the free acids (HL_n), which followed the trend of $HL_3 < HL_2 < HL_1 < HL_u$. The order of p$K_a$ for the TFM-modified (DTP+H) acids was opposite of what would be expected based on the e^--withdrawing effects of the TFM group, suggesting that secondary factors influence the pK_a and nucleophilicity. The relative nucleophilicities of the DTP anions were evaluated by forming metal−mixed ligand complexes in a trapped ion mass spectrometer and then fragmenting them using competitive collision induced dissociation. On the basis of these experiments, the unmodified L_u^- anion was the strongest nucleophile. Comparing the TFM derivatives, the *bis*(*ortho*-TFM) derivative L_1^- was found to be the strongest nucleophile, while the *bis*(*meta*-TFM) L_3^- was the weakest, a trend consistent with the pK_a calculations. DFT modeling of the Na^+ complexes suggested that the elevated cation affinity of the L_1^- and L_2^- anions was due to donation of electron density from fluorine atoms to the metal center, which was occurring in rotational conformers where the TFM moiety was proximate to the Na^+-dithiophosphinate group. Competitive dissociation experiments were performed with the dithiophosphinate anions complexed with europium nitrate species; ionic dissociation of these complexes always generated the TFM-modified dithiophosphinate anions as the product ion, showing again that the unmodified L_u^- was the strongest nucleophile. The Eu(III) nitrate complexes also underwent redox elimination of radical ligands; the tendency of the ligands to undergo oxidation and be eliminated as neutral radicals followed the same trend as the nucleophilicities for Na^+, viz. $L_3^- < L_2^- < L_1^- < L_u^-$.

Introduction

An ongoing challenge in nuclear separation science is selective complexation of various +3 cations.[1] Of particular interest are the separations of the so-called minor actinides Am^{3+} and Cm^{3+} from other fission products, most notably lanthanide^{3+} cations, which is motivated by the fact that these actinides have very long half-lives and are major contributors to the heat load and radioactivity in geologic repositories.[2,3] Chemically, these separations, which rely on selective complex formation, are difficult: at low pH values in

* To whom correspondence should be addressed. E-mail: garold.gresham@inl.gov.
[†] Wichita State University.
[‡] Idaho National Laboratory.
[§] Université Paul Verlaine–Metz.

(1) Nash, K. L. *Solvent Extr. Ion Exch.* **1993**, *11*, 729.
(2) Ogawa, T.; Minato, K.; Okamoto, Y.; Nishihara, K. *J. Nucl. Mater.* **2007**, *360*, 12.
(3) Salvatores, M. *Nucl. Eng. Des.* **2005**, *235*, 805.

10.1021/ic7020897 CCC: $40.75
Published on Web 03/05/2008

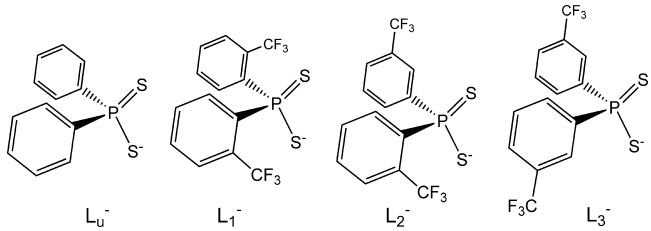

Figure 1. Structures of the diphenyldithiophosphinate ligands.

noncomplexing solutions, the actinide and lanthanide^{3+} cations act as very aggressive Lewis acids which have very similar ionic radii,[1] and so development of selective complexation schemes that have utility for liquid–liquid separations is challenging. This objective motivated the development of the "trivalent actinide-lanthanide separation by phosphorus reagent extraction from aqueous complexes" (TALSPEAK) process, which is a viable method of extraction but generates large quantities of aqueous waste in achieving separation.[4,5] Accordingly, research has focused on identifying new ligands that have higher selectivity for actinide^{3+} versus lanthanide^{3+} cations, with concurrent fast separation kinetics.[1,4–6] A particularly intriguing development is the emergence of dithiophosphinate ligands, that are softer donor ligands compared to oxygen donors, and have the ability to form ligand–metal bonds with significant covalent character.[7–9] The best example of this chemistry is perhaps *bis*(2,4,4,-trimethylpentyl)dithiophosphinic acid (Cyanex 301), which has been widely investigated for *f*-element separation efficacy.[7,9,10]

Recently, in our laboratories, a series of diphenyldithiophosphinate (DTP) derivatives have been synthesized and have shown excellent promise for effecting highly selective separations of Am^{3+} from Eu^{3+}.[11] The DTP ligands were modified by addition of trifluoromethyl (TFM) groups to the phenyl rings. A total of four derivatives were studied (Figure 1): unmodified DTP (L_u^-), *bis*(*ortho*-trifluoromethylphenyl)dithiophosphinate (L_1^-), (*ortho*-trifluoromethylphenyl)(*meta*-trifluoromethylphenyl)dithiophosphinate (L_2^-), and *bis*(*meta*-trifluoromethylphenyl)dithiophosphinate (L_3^-). The compounds were synthesized with the objective of separating Am^{3+} from lanthanide^{3+} cations, and in separation experiments, both derivatives L_1^- and L_2^- were shown to partition Am^{3+} into an organic phase, while Eu^{3+} partitioning was much more modest.[11] The L_1^- and L_2^- derivatives displayed exceptionally high separation factors, approaching or exceeding 10^5. In contrast, the Am^{3+}/Eu^{3+} separation factor for the L_3^- derivative was substantially lower. Thus from a phenomenological perspective, both L_1^- and L_2^- showed substantial promise for much improved Am^{3+} separations, but the details of the physical interactions responsible for preferential complex formation are not understood.

Scheme 1. Generalized Competitive Dissociation of Na^+−Mixed Ligand Anionic Species

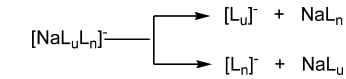

Variations in separation efficiency observed when comparing the ligands may be correlated with differences in the acidities of the protonated DTP ligands. A priori, we expected that the phenyl moieties most capable of withdrawing electron density from the dithiophosphinate (DTP) group would induce increased acidity (and conversely would produce a less nucleophilic conjugate base). This should be the isomers containing the *ortho*-TFM moieties, which would be expected to be better e^--withdrawing groups on account of a more effective inductive effect due to the closer proximity of the TFM group (compared to the meta position),[12,13] and should be ortho/para activating if resonance is involved. Experimentally, it is very difficult to investigate the acidity (or nucleophilicity) of the DTP species in the condensed phase, because of limited solubility in most solvents with the exception of the water-immiscible polar solvent trifluoromethylphenyl sulfone (referred to as FS-13 in the *f*-element separations vernacular) and low molecular weight alcohols. Therefore, we approached the problem of evaluating (DTP+H) acidity using density functional theory (DFT) calculations.

The acidity calculations were experimentally complemented using measurements of relative nucleophilicities via competitive dissociation reactions of ionic complexes isolated in the gas phase environment of a trapped ion mass spectrometer.[14] Complexes were readily formed by electrospray ionization that had the general composition of $[NaL_uL_{n=1,2,3}]^-$, which were then isolated by the mass-to-charge ratio using ion ejection in a quadrupole ion trap.[15] The $[NaL_uL_{n=1,2,3}]^-$ (note that, in this nomenclature, the subscript identifies the particular TFM derivative) complexes were then collisionally activated, which is accomplished by increasing their average kinetic energy inside the trapped ion mass spectrometer.[15] The resulting hyperthermal collisions with a neutral bath gas (He in the present case) partition the increased kinetic energy into internal vibrational and rotational modes, which dissociates the complexes. Negatively charged L_u^- and $L_{n=1,2,3}^-$ fragment ions are formed in this manner and detected by the mass spectrometer, concurrent with $ML_{n=1,2,3}$ and ML_u neutrals that are not detected (Scheme 1). In general, the most abundant fragment ion produced corresponds to the weakest nucleophile, and the ratio of the two dissociation pathways can provide a

(4) Mathur, J. N.; Murali, M. S.; Nash, K. L. *Solvent Extr. Ion Exch.* **2001**, *19*, 357.
(5) Nash, K. L.; Barrans, R. E.; Chiarizia, R.; Dietz, M. L.; Jensen, M. P.; Rickert, P. G. *Solvent Extr. Ion Exch.* **2000**, *18*, 605.
(6) Nash, K. L.; Jensen, M. P. *Sep. Sci. Technol.* **2001**, *36*, 1257.
(7) Ionova, G.; Ionov, S.; Rabbe, C.; Hill, C.; Madic, C.; Guillaumont, R.; Krupa, J. C. *Solvent Extr. Ion Exch.* **2001**, *19*, 391.
(8) Pattee, D. M., C.; Faure, A.; Chachaty, C. *J. Less Common Metals* **1986**, *122*, 295.
(9) Hill, C.; Madic, C.; Baron, P.; Ozawa, M.; Tanaka, Y. *J. Alloys Compd.* **1998**, *271–273*, 159.
(10) Zhu, Y.; Chen, J.; Jiao, R. *Solvent Extr. Ion Exch.* **1996**, *14*, 61.
(11) Klaehn, J. R.; Peterman, D. R.; Tillotson, R. D.; Luther, T. A.; Harrup, M. K.; Law, J. D.; Daniels, L. M. *Inorg. Chim. Acta*, submitted for publication.
(12) Exner, O.; Bohm, S. *Phys. Chem. Chem. Phys.* **2004**, *6*, 3864.
(13) Hansch, C.; Leo, A.; Taft, R. W. *Chem. Rev.* **1991**, *91*, 165.
(14) Cooks, R. G.; Patrick, J. S.; Kotaiho, T.; McLuckey, S. A. *Mass Spectrom. Rev.* **1994**, *13*, 287.
(15) Todd, J. F. J. *Practical Aspects of Ion Trap Mass Spectrometry*; CRC Press: New York, 1995; Vol. *1*, p 4.

qualitative evaluation of the relative nucleophilicities of the two ligands, provided entropy changes are comparable for both pathways.

Relative Na^+ nucleophilicities were experimentally generated in this fashion, and insight into factors responsible for observed binding preferences were gained using DFT to model coordination complexes of DTP anions with Na^+. In addition to the experiments with the mixed ligand Na^+ complexes, competitive dissociation of europium nitrate−mixed ligand complexes $[Eu(NO_3)_2L_uL_{n=1,2,3}]^-$ were also studied to gain a more comprehensive assessment of ligand nucleophilicity relative to a metal center containing an *f*-element.

Experimental Details

An axial nanospray ion source fitted with a 30 μm i.d. fused-silica PicoTip emitter (New Objective, Woburn, MA) was used to introduce the mixed ligand complexes into an LCQ Deca IT mass spectrometer (Thermo Fisher Scientific, San Jose, CA). The low-flow nanospray source was operated at a spray voltage of 1.6 ± 0.2 kV. Electrical contact was made directly to the mobile phase at the tee-fitting holding the emitter. Competitive CID reactions were carried out using established procedures described elsewhere, such that the excitation energy was increased until the parent ion was reduced to 10% of its original value.[16−18] Standard solutions of sodium chloride (NaCl) and europium (III) nitrate pentahydrate ($Eu(NO_3)_3 \cdot 5H_2O$) were prepared by dissolving the salt in an appropriate amount of analytical grade methanol (MeOH) or ethanol (EtOH) to achieve a concentration of 0.1 M. The dithiophosphinate ligands were synthesized in house,[11] and stock solutions were made by dissolving an appropriate amount of dithiophosphinate ligand in 1 mL of MeOH, such that the final concentration was equimolar with that of the metal cation. Spray solutions were created by mixing 50 μL of standard salt solution, 8.52 μL of HL_u solution, and 3.23, 5.85, or 16.1 μL of HL_1, HL_2, and HL_3, respectively, and then, MeOH or EtOH was added to bring the solutions to a volume of 1 mL. These solutions were then infused into the nanospray source using the incorporated syringe pump at a flow rate of 200−800 nL/min. The atmospheric pressure ionization stack settings for the LCQ (lens voltages, quadrupole and octapole voltage offsets, etc.) were optimized for maximum ion transmission to the ion trap mass analyzer by using the autotune routine within the LCQ Tune program. To ensure maximum yield of solvated metal–ligand anion complexes, the heated capillary temperature was maintained at 125°. Helium was used as the bath/buffer gas to improve the trapping efficiency and as the collision gas for CID experiments.

To resolve issues with compositional uncertainty, a selected set of mass spectra were acquired in negative detection mode using an electrospray ionization-Fourier transform-ion cyclotron resonance (ESI-FT-ICR) mass spectrometer (MS)[19,20] (IonSpec, Lake Forest, CA) equipped with an actively shielded 9.4-T superconducting magnet (Cryomagnetics, Oak Ridge, TN). Ions were generated by spraying an ∼100 μM solution of the sodium−ligand solutions, skimming ions from the spray into an RF-only hexapole before transfer to the FT-ICR cell. The ion guide was optimized for an *m*/*z* 850 ion and allowed ions in the 300–1500 *m*/*z* range to be efficiently transferred into the FT-ICR cell. After transfer, ions were trapped in the FT-ICR cell with a −0.5 V trapping potential. Then, *m*/*z* 100−2500 ions were excited by the application of an arbitrary excitation wave function on the excitation plates. The resulting image current was detected, amplified, digitized, apodized (Blackman), and Fourier-transformed to produce a mass spectrum. The signal was sampled during 2.097 s with 2 048 000 data points. The average mass measurement accuracy obtained was typically close to 1.3 ppm, and the mass resolution at *m*/*z* 1200 close to 100 000.

Density functional calculations were performed with the Gaussian 03 program.[21] For the pK_a calculations, both neutral and anionic species were calculated using DFT[22] at the B3LYP/6-311G(d,p) level of theory.[23,24] Structures including Na^+ were calculated using the 3-21G* basis set, and a subset was performed using the larger 6-311G+(d,p). All calculated structures are true minima, i.e. no imaginary frequencies. The solvated species were calculated with the CPCM continuum solvation method.[25,26] The default Gaussian 03 dielectric constant for water was used for all calculations, $\varepsilon = 78.39$. This parameter was not modified, since it has been shown that pK_a is insensitive to minor changes in the dielectric constant.[27] Liptak et al.[28] found that calculating the solvation correction using gas phase geometries did not yield accurate pK_a values, especially if the anions were not optimized in the solution phase, due to charge redistribution. In this work, all solution phase vibrational data was calculated from solution phase optimized structures. All energetic data include zero point energy and an enthalpy correction (from 0 to 298 K).

Ligand pK_a values were determined using the following equations (eqs 1−4). In a general deprotonation reaction, AH dissociates into A^- and H^+, as in eq 1:

$$AH \rightarrow A^- + H^+ \quad (1)$$

The pK_a is given by eq 2, where $\Delta G_{AH,aq}$ is the gas phase free energy with a correction for solvation, as shown in eq 3 and the expanded equation (eq 4).

$$pK_a = \Delta G_{AH,aq}/2.303RT \quad (2)$$

$$\Delta G_{AH,aq} = \Delta G_{AH,g} + \Delta\Delta G_{AH,s} \quad (3)$$

(16) Hanna, D.; Silva, M.; Morrison, J.; Tekarli, S.; Anbalagan, V.; Van Stipdonk, M. J. *J. Phys. Chem. A* **2003**, *107*, 5528.
(17) Perera, B. A.; Gallardo, A. L.; Barr, J. M.; Tekarli, S. M.; Anbalagan, V.; Talaty, E. R.; Van Stipdonk, M. J. *J. Mass Spectrom.* **2002**, *37*, 401.
(18) Van Stipdonk, M.; Anbalagan, V.; Chien, W.; Gresham, G.; Groenewold, G.; Hanna, D. *J. Am. Soc. Mass Spectrom.* **2003**, *14*, 1205.
(19) Marshall, A. G. *Acc. Chem. Res.* **1985**, *18*, 316.
(20) Marshall, A. G.; Hendrickson, C. L.; Jackson, G. S. *Mass Spectrom. Rev.* **1998**, *17*, 1.
(21) Frisch, M. J.; Trucks, G. W.; Schlegel, H. B.; Scuseria, G. E.; Robb, M. A.; Cheeseman, J. R.; Montgomery, J. A. J.; Vreven, T.; Kudin, K. N.; Burant, J. C.; Millam, J. M.; Iyengar, S. S.; Tomasi, J.; Barone, V.; Mennucci, B.; Cossi, M.; Scalmani, G.; Rega, N.; Petersson, G. A.; Nakatsuji, H.; Hada, M.; Ehara, M.; Toyota, K.; Fukuda, R.; Hasegawa, J.; Ishida, M.; Nakajima, T.; Honda, Y.; Kitao, O.; Nakai, H.; Klene, M.; Li, X.; Knox, J. E.; Hratchian, H. P.; Cross, J. B.; Adamo, C.; Jaramillo, J.; Gomperts, R.; Stratmann, R. E.; Yazyev, O.; Austin, A. J.; Cammi, R.; Pomelli, C.; Ochterski, J. W.; Ayala, P. Y.; Morokuma, K.; Voth, G. A.; Salvador, P.; Dannenberg, J. J.; Zakrzewski, V. G.; Dapprich, S.; Daniels, A. D.; Strain, M. C.; Farkas, O.; Malick, D. K.; Rabuck, A. D.; Raghavachari, K.; Foresman, J. B.; Ortiz, J. V.; Cui, Q.; Baboul, A. G.; Clifford, S.; Cioslowski, J.; Stefanov, B. B.; Liu, G.; Liashenko, A.; Piskorz, P.; Komaromi, I.; Martin, R. L.; Fox, D. J.; Keith, T.; Al-Laham, M. A.; Peng, C. Y.; Nanayakkara, A.; Challacombe, M.; Gill, P. M. W.; Johnson, B.; Chen, W.; Wong, M. W.; Gonzalez, C.; Pople, J. A. *Gaussion 03*, revision C.02; Gaussian, Inc.: Wallingford, CT, 2004.
(22) Parr, R. G.; Yang, W. *Density Functional Theory of Atoms and Molecules*; Oxford University Press: New York, 1989.
(23) Becke, A. D. *Phys. Rev. A* **1988**, *38*, 3098.
(24) Lee, C. T.; Yang, W. T.; Parr, R. G. *Phys. Rev. B* **1988**, *37*, 785.
(25) Barone, V.; Cossi, M. *J. Phys. Chem. A* **1998**, *102*, 1995.
(26) Cossi, M.; Rega, N.; Scalmani, G.; Barone, V. J. *Comp. Chem.* **2003**, *24*, 669.
(27) Jang, J. H.; Sowers, L. C.; Çağin, T.; Goddard, W. A., III *J. Phys. Chem. A* **2001**, *105*, 274.
(28) Liptak, M. D.; Shields, G. C. *J. Am. Chem. Soc.* **2001**, *123*, 7314.

$$\Delta G_{AH,aq} = \Delta G_{A^-,g} + \Delta G_{A^-,s} + \Delta G_{H^+,g} + \Delta G_{H^+,s} - \Delta G_{AH,g} - \Delta G_{AH,s} \quad (4)$$

The gas phase $\Delta G_{AH,g}$ and $\Delta G_{A^-,g}$ are determined from the total gas phase energy of the molecule including the zero point energy and a thermal correction (from 0 to 298 K), obtained from the vibrational analysis. Recent experimental values that have been used for $\Delta G_{H^+,g}$ and $\Delta G_{H^+,s}$ are −6.28 and −263.98 kcal/mol, respectively.[29–31] An added term ($-RT$ ln(24.46)) is used to account for the change in concentration units between gas phase and aqueous calculations.

Results and Discussion

DFT Calculations of pK_a Values. In order to calculate pK_a, the geometry must be accurately described first. Figure 2 shows the calculated structures for the free acids HL_u, HL_1, HL_2, and HL_3. Although there is potential for change of the dihedral angle that includes the acidic proton, the lowest energy configuration has the proton in the cis configuration, being partially shared between the two sulfur atoms. The energy difference between this configuration and the other possibility, where the proton points away from the sulfide, is ∼1–2 kcal/mol. In both ligands with an *ortho*-TFM group (free acids of L_1^- and L_2^-), the lowest energy configuration of the TFM group is behind the phosphorus, as opposed to the complexes calculated with sodium, vide infra, where the *ortho*-TFM rotates and interacts with the sodium. The calculated barrier to rotation is 19.6 kcal/mol for HL_1 and 8.8 kcal/mol for HL_2. The barrier is more than double that for HL_1 than HL_2, due to the second *ortho*-TFM group. As one phenyl ring rotates, the second also has to rotate to prevent close contacts. In HL_2, the *meta*-TFM phenyl group is less sterically hindered than the second *ortho*-TFM phenyl group in HL_1; therefore, the *meta*-TFM phenyl group does not have to rotate as much and requires less energy to rotate. A crystal structure has been generated for HL_1, which showed that the *ortho*-TFM groups are positioned behind the phosphorus atom, opposite the S atoms,[11] which is consistent with the DFT structures shown in Figure 2 for HL_1 and HL_2. Table 1 lists the important geometrical parameters for the crystal structure and calculated structures for HL_u, HL_1, HL_2, and HL_3. The calculated and experimental structures were in excellent agreement in terms of bond lengths and angles, with the exception of the P−S bond length. Due to hydrogen-bonding in the crystal structure,[11] which is not explicitly included in the calculated structure, the P−S bond length is shortened in the condensed-phase structure.

The pK_a values were calculated for HL_u, HL_1, HL_2, and HL_3 molecules at 2.18, 1.72, 1.52, and 0.20, respectively. Due to their extremely low solubility in water, pK_a values for these acids have not been measured experimentally, and so, the pK_a of the *bis*-alkyl-DTP acid Cyanex 301 was used to evaluate computational accuracy. The DFT-calculated

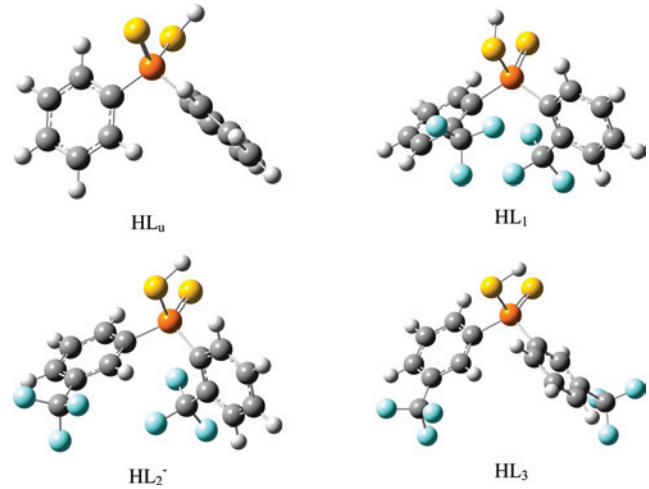

Figure 2. Calculated structures for HL_u, HL_1, HL_2, and HL_3.

value for Cyanex 301 is 3.42, which is in reasonable agreement with experimentally measured values of 2.61[32] and 2.84.[33] Of these two reported measurements, 2.84 is judged to be the more reliable value based on the method used, making the difference between experimental and theoretical values equal to 0.58. Gutowski and Dixon have pointed out that there are drawbacks to calculating pK_a using eqs 1−4[34] and recommended improving accuracy by referencing calculated pK_a values to an established reference acid. This would be difficult to do in the present case, given that there is only one experimental data point for this class of compounds. Nevertheless, the error in the calculated pK_a value for Cyanex 301 provides confidence that the pK_a of HL_3 is certainly lower than the other three derivatives, and suggests that the trending is correct as well, even though a more rigorous accuracy evaluation will have to wait until more experimental validation is available.

As discussed above, one would expect the free acid of L_1^- to be the most acidic, based on the inductive effect of the TFM group in the *ortho*-position on the phenyl ring. This reasoning and the overall e^--donating characteristic of the phenyl ring, led to the expectation that the trend in pK_a values of the free acids would follow the order $HL_1 < HL_2 < HL_3 < HL_u$. In contrast, the trend seen in the DFT-calculated pK_a values for the free acids is the exact opposite, $HL_3 < HL_2 < HL_1 < HL_u$, suggesting that electron-withdrawing effects are not the only factors that influence the pK_a values. We hypothesize that the *ortho*-TFM groups are causing steric strain in HL_1 and, to a lesser degree, HL_2 that is affecting the pK_a values. This idea is supported by the C−P−C angle in the structure of the HL_1 free acid, which is wider than the other ligands (112.8° vs ∼106°). This is not the case in the HL_2 free acid, where the *meta*-TFM phenyl group has more steric freedom, thus allowing it to relieve the strain in the C−P−C angle. In addition, the P−C bond length is longer when an *ortho*-TFM group is present, and the S−P−S angle decreases by roughly 2° for each *ortho*-TFM group.

(29) Kelly, C. P.; Cramer, C. J.; Truhler, D. G. *J. Phys. Chem. B* **2006**, *110*, 16066.
(30) Tissandier, M. D.; Cowen, K. A.; Feng, W. Y.; Gundluach, E.; Cohen, M. H.; Earhart, A. D.; Coe, J. V.; Tuttle, T. R. *J. Chem. Phys.* **1998**, *102*, 7787.
(31) Topol, I. A.; Tawa, G. J.; Burt, S. K.; Rashin, A. A. *J. Chem. Phys.* **1999**, *111*, 10998.
(32) Jia, Q.; Zhan, C.; Li, D.; Niu, C. *Sep. Sci. Technol.* **2004**, *39*, 1111.
(33) Xun, F.; Yahong, X.; Shuyun, X.; Shaona, Z.; Zhengshui, H. *Solvent Extr. Ion Exch.* **2002**, *20*, 331.
(34) Gutowski, K. E.; Dixon, D. A. *J. Phys. Chem. A.* **2006**, *110*, 12044.

Table 1. Comparison of DFT-Calculated Bond Distances and Angles for HL_u, HL_1, HL_2, and HL_3, with Experimental Geometric Parameters Measured Using X-ray Crystallography

ligand	P—S (Å)	P═S (Å)	P—C (Å)[a]	P···F (Å)[a]	P—C (Å)[a]	<C—P—C (°)	<S—P—S (°)
HL_u, DFT	2.17	1.96	1.83		1.83	106.6	114.9
			1.84		1.83		
HL_1, DFT	2.17	1.97	1.86	3.08	1.87	112.8	111.6
			1.87	2.94	1.86		
HL_2, DFT	2.17	1.96	1.83	2.98	1.83	107.0	113.0
			1.87		1.87		
HL_3, DFT	2.16	1.96	1.84		1.84	106.0	115.7
			1.84		1.84		
HL_1, crystal structure	2.09	1.96	1.84	3.12	1.84	113.5	113.1
			1.85	2.97	1.85		

[a] Multiple values are given for molecules containing two bonds that are atomistically the same, but have different calculated bond distances.

Although none of these changes by themselves are very large, taken together they may be enough to reduce the inductive e^--withdrawing efficiency of the *ortho*-TFM groups. A second hypothesis is that the *ortho*-TFM groups are back-donating e^- density to the thiophosphoryl via close interaction of the F atoms with the phosphorus center. This is supported by P—F bond distances, which are as short as 2.94 Å (Table 1), but we are aware of no precedent for such an interaction in a P(V) system and nuclear magnetic resonance spectra of the ligands do not show P—F coupling.[11] Unfortunately, calculated Mulliken atomic charges support both hypotheses. Calculated charges for fluorine indicate that a through space interaction with phosphorus may be real. The trend is more obvious with the anionic ligands, although the trend is still evident in the neutral ligands. The fluorine closest to the phosphorus has less e^- density than the other two fluorines on the CF_3 group. As an example, the fluorine charges for L_1^- in the gas phase are −0.181 and −0.192 for the fluorines closest to the phosphorus, and −0.221, −0.238, −0.214, and −0.243 for the other four fluorines. This is also the case for L_2^-, where only one fluorine is near the phosphorus. The Mulliken atomic charges for phosphorus (both gas and solution phase, as well as neutral and anionic) indicate that L_3^- has the least e^- density, with the order $L_3^- < L_2^- < L_1^-$. This is likely due in part to the lack of proximal fluorine atoms in L_3^-, although a diminished e^--withdrawing effect from the *meta*-TFM groups (compared to L_2^- and L_1^-) may also be contributing. A full list of Mulliken charges are in the Supporting Information.

Nucleophilicites from Dissociation of DTP Complexes with Na^+. As noted above, experimental measurement of the acidities of the DTP free acids is severely hampered by solubility problems. However, we found that metal−mixed ligand complexes could be readily formed using electrospray ionization mass spectrometry, enabling competitive collision induced dissociation experiments. The negative ion electrospray ionization mass spectra of Na^+ dissolved with each of the three TFM-derivatized ligands are qualitatively identical to one another. The Na^+ cation was utilized because it provided a simplified charge center for modeling purposes and was easily formed in the electrospray. Further, more recent experiments have shown that the DTP ligands will form organic soluble complexes with Na^+, and hence, it is of interest in its own right. At lower mass ranges, ions at *m/z* 249 and 385 correspond to *bis*(phenyl)dithiophosphinate L_u^- and one of the TFM derivatives L_n^-, respectively (Figure 3). The ions at *m/z* 521, 657, and 793 constitute a series corresponding to $[Na(L_u)_2]^-$, $[Na(L_u)(L_{n=1,2,3})]^-$, and $[Na(L_{n=1,2,3})_2]^-$, respectively. In addition, there were higher mass ions that were identified on the basis of accurate mass measurements (Table 2) using the FT-ICR-MS and correspond to metal–ligand complexes containing Fe^{2+}, Ca^{2+}, and Cu^+: the origin of the metals contained in these complexes was not identified but may involve metal components encountered in the ESI instruments. When the sampling cone of the ESI instrument was cleaned, a black, probably sulfidic residue was observed, indicating that the dithiophosphinate ligands were interacting with the metal surfaces. The Fe^{2+}-bearing complexes were observed in spectra from both the quadrupole ion trap and in the FT-ICR-MS; however, the Cu^+ complex was only observed in the FT-ICR-MS. The appearance of these ions and their great abundance is indicative of the high affinity the dithiophosphinate ligands have for metals and of the fact that complexes with transition metals are probably much more tightly bound compared to complexes with the Group I alkali Na^+. This suggests that complexes with lanthanide metals will be much more tightly bound as well compared to complexes with the Group I alkali Na^+.

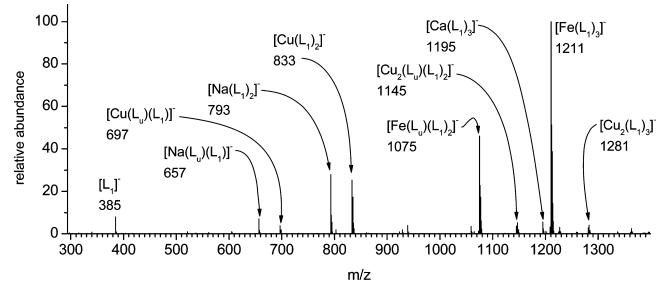

Figure 3. ESI-MS-1 spectrum of a mixture of L_1^- and L_u^- dithiophosphinate ligands generated by spiking the spray solution with NaCl. Spectra were acquired using the FT-ICR-MS instrument.

Table 2. Accurate Masses, Compositions, Measured Using the ESI-FT-ICR-MS

measured	theoretical	error (ppm)	composition
384.9714	384.9715	−0.18	$[((CF_3)C_6H_4)_2PS_2]^-$
656.9574	656.9574	0.02	$[((CF_3)C_6H_4)_2PS_2]Na[(C_6H_5)_2PS_2)]^-$
696.8984	696.8972	1.68	$[((CF_3)C_6H_4)_2PS_2]Cu[(C_6H_5)_2PS_2)]^-$
792.9331	792.9322	1.19	$Na[((CF_3)C_6H_4)_2PS_2]_2^-$
832.873	832.872	1.21	$Cu[((CF_3)C_6H_4)_2PS_2]_2^-$
1058.901	1058.901	0.15	$[(C_6H_5)_2PS_2)]Ca[((CF_3)C_6H_4)_2PS_2]_2^-$
1074.871	1074.873	−2.50	$[(C_6H_5)_2PS_2)]Fe[((CF_3)C_6H_4)_2PS_2]_2^-$
1194.88	1194.876	3.51	$Ca[((CF_3)C_6H_4)_2PS_2]_3^-$
1210.848	1210.848	−0.13	$Fe[((CF_3)C_6H_4)_2PS_2]_3^-$

Scheme 2. Competitive Dissociation Reactions of the $[Na(L_u)(L_1)]^-$

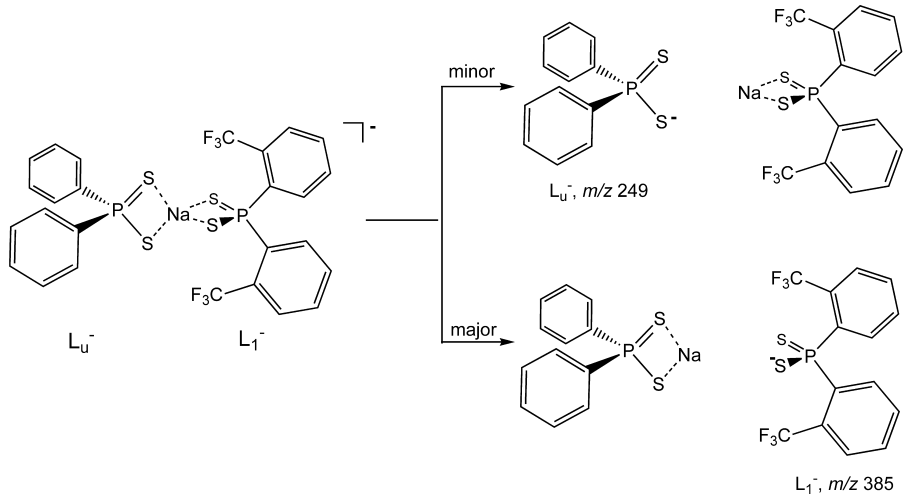

Table 3. Relative Percent Elimination of NaL_n and NaL_u Neutral Molecules from Mixed $[Na(L_n)(L_u)]^-$ Complexes

mixed ligand complex	elimination of NaL_u (formation of L_n^-)	elimination of NaL_n (formation of L_u^-)
$[Na(L_u)(L_1)]^-$	99.57	0.43
$[Na(L_u)(L_2)]^-$	99.99	0.01
$[Na(L_u)(L_3)]^-$	100	$<6 \times 10^{-6}$

Table 4. Loss Ratios $(-NaL_n)/(-NaL_u)$ in Dissociation of the Mixed Complexes $[Na(L_n)(L_u)]^-$

loss ratio	parent depletion to 10%
$(-NaL_1)/(-NaL_u)^a$	4.3×10^{-3}
$(-NaL_2)/(-NaL_u)^a$	1.0×10^{-4}
$(-NaL_3)/(-NaL_u)^a$	$<1.0 \times 10^{-6}$
$(-NaL_1)/(-NaL_2)^b$	4.3×10^1
$(-NaL_2)/(-NaL_3)^b$	$>1.0 \times 10^2$

[a] Ratios calculated from a direct measurement, single experiment. [b] Ratio of ratios from two different experiments.

The ion at *m/z* 657 is of particular interest, as it corresponds to $[Na(L_u)(L_{n=1,2,3})]^-$. Isolation and activation of this ion in the quadrupole ion trap resulted in collision induced dissociation, which in each case produced predominantly anion products at *m/z* 385, corresponding to the TFM conjugate bases L_n^-, formed by elimination of neutral NaL_u. This indicates that L_u^- has a higher intrinsic cation affinity and, thus, is a stronger nucleophile than are any of the TFM-modified L_n^- anions, because it remains bound to the metal ion after the dissociation reaction. Careful examination of the spectra of complexes at *m/z* 657 containing the *bis*(*ortho*-TFM) L_1^- and (*ortho*-TFM)(*meta*-TFM) L_2^- ligands showed low abundance ions at *m/z* 249, that corresponded to L_u^-. Thus, in these cases, elimination of L_u^- was to a minor extent competitive with elimination of the TFM conjugate bases L_1^- and L_2^-. The competitive reactions for the $[Na(L_u)(L_1)]^-$ complex are shown in Scheme 2, and the percent abundances of the different elimination channels are presented in Table 3, while the loss ratios are presented in Table 4.

The relative propensity for elimination can be described by the ratio of the elimination of the TFM ligands L_n^- to the elimination of the unmodified diphenyldithiophosphinate ligand L_u^- (Table 4). None of the TFM derivatives are effective at competing with the unmodified diphenyldithiophosphinate L_u^- for Na^+. However, comparisons of the $(-NaL_n)/(-NaL_u)$ elimination ratios show a trend $L_3^- < L_2^- < L_1^-$, indicating that the *bis*(*ortho*-trifluoromethylphenyl) ligand L_1^- binds more tenaciously than the *ortho,meta*-ligand L_2^-, which in turn is more strongly binding than the *bis*(*meta*)-derivative L_3^-. The magnitude of these preferences can be quantified in an empirical fashion by dividing the $(-NaL_n)/(-NaL_u)$ ratios (Table 4), which shows that, during dissociation, Na^+ remaining bound to L_1^- is preferred by a factor of 43 compared to L_2^-, which in turn is preferred by a factor greater than 100 compared to L_3^-. On the basis of these results, the intrinsic nucleophilicities of the L_n^- ligands are predicted to follow the order $L_3^- < L_2^- < L_1^-$, and conversely, the acidity of the free acids of the L_n^- ligands should be the opposite, viz., $HL_1 < HL_2 < HL_3$. This trend is in agreement with the DFT predictions of pK_a values.

The fact that L_1^- is a stronger nucleophile than L_3^- is counterintuitive based on reactivity alterations expected solely on electronic effects due to TFM substitution on the aromatic rings. TFM is a powerful electron-withdrawing group,[35] operating to remove electron density from the aromatic ring, and hence from the dithiophosphinate $(-PS_2^-)$ moiety responsible for complexing metal cations. Removal of electron density from $-PS_2^-$ should reduce ligand nucleophilicity, and in fact, this is observed: the nucleophilicity of all three of the TFM derivatives are much lower than the unmodified diphenyldithiophosphinate L_u^-. The TFM moiety functions principally in an inductive fashion, which means that the closer it is to the $-PS_2^-$ group, the more effective it should be in decreasing electron density localized on $-PS_2^-$. On the basis of this argument, the *bis*(*ortho*-trifluoromethylphenyl)dithiophosphinate L_1^- should be more effective at decreasing nucleophilicity than either the (*ortho*)(*meta*)- or the *bis*(*meta*)-derivatives. The fact that the opposite trend is observed suggests that, as in the case of the free acids, another factor is at work augmenting L_1^- nucleophilicity.

DFT modeling was employed to attempt to gain insight into the nature of L_n^- binding with metal cations. DFT at the B3LYP/3-21 g* level for the $[NaL_1]$ complex revealed

(35) Hansch, C.; Leo, A.; Taft, R. W. *Chem. Rev.* **1991**, *91*, 165.

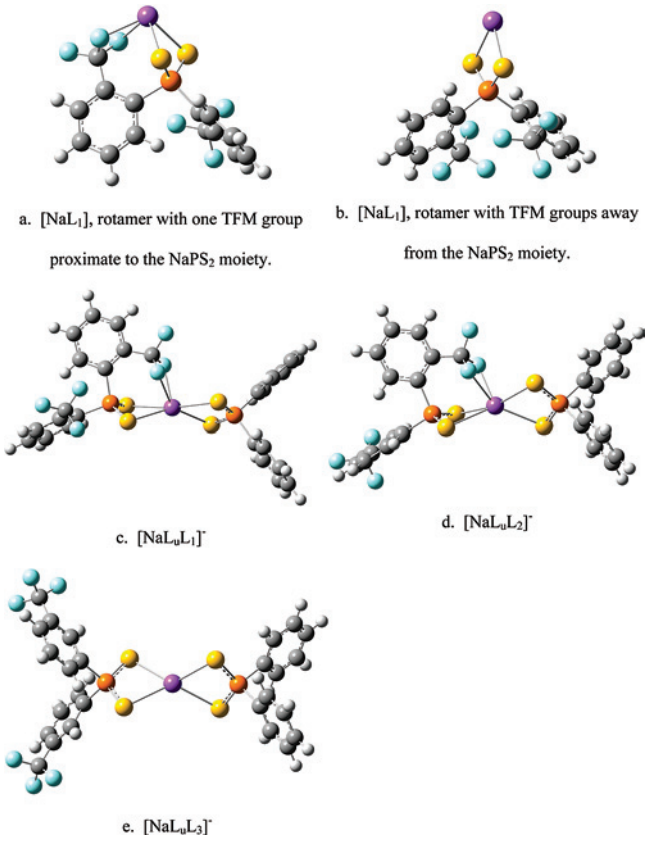

Figure 4. Structures of Na^+ complexes with the DTP ligands, calculated at the B3LYP/3-21 g* level

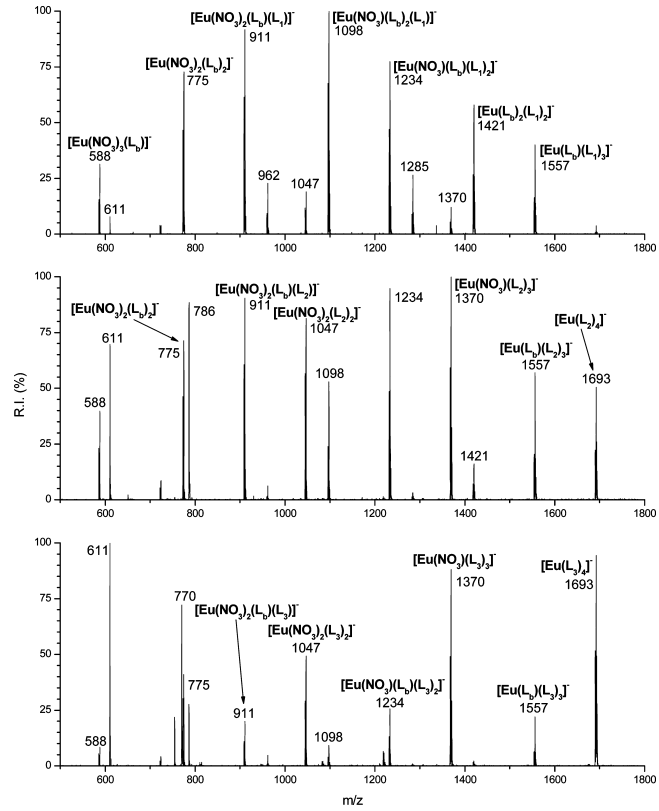

Figure 5. Negative ESI MS-1 spectrum of europium nitrate and L_u^-, in conjunction with L_1^- (top), L_2^- (center), and L_3^- (bottom). Spectra were acquired using the quadrupole ion trap instrument.

several rotational conformers that were stable. The most stable rotamers had a structure in which the *ortho*-TFM group was rotated proximate to the Na^+ center (Figure 4a). The Na−F distance was 2.27 Å in this structure, and energetic calculations indicated that it was 14–16 kcal/mol more stable than an alternative rotamer in which the TFM group was rotated away from the $Na-PS_2$ moiety (Figure 4b). In this latter rotamer, no Na−F interaction occurs and the Na^+ occupies a coplanar position within the PS_2^- cleft. Bond distances were used to determine Na and F interactions, which are listed in the Supporting Information. In contrast, Na−F interactions displace Na^+ from this position, producing a structure in which Na^+ is situated in a "pocket" consisting of two S and two F donor atoms (Figure 4a). We repeated the calculations for the $[NaL_1]$ complex using the B3LYP functional and the larger 6-311+g(d,p) basis set and found the same structural preferences, although the energetic differences between the rotamers was not as great. Analogous results were obtained in modeling the $[NaL_2]$ complex, viz., of multiple possible rotamers, structures in which the TFM moiety was rotated such that interactions with Na^+ were more stable by 16–17 kcal/mol. In contrast, results for the $[NaL_3]$ complex showed no significant preference for different rotamers, and Na^+ was nearly coplanar with the PS_2 moiety (similar to the configuration in Figure 4b), observations consistent with the fact that the TFM groups cannot interact with the metal cation when occupying the meta position.

The preference for the $TFM-PS_2$ pocket was also seen in the calculated structures of the full complexes. The most stable structure calculated for the $[NaL_uL_1]^-$ complex had the TFM moiety rotated proximate to Na^+, which pulled the cation out of the PS_2 plane (Figure 4c). The PS_2 group of L_u^- was rotated so as to minimize repulsion with not only the PS_2^- of L_1^- but also that of the TFM group. Analogous results were calculated for the $[NaL_uL_2]^-$ complex: in this case, a rotamer in which the TFM group was rotated away from Na^+ was located as a local minimum which was 10 kcal/mol higher in energy than the rotamer with the $TFM-PS_2$ pocket (Figure 4d). The structure calculated for the $[NaL_uL_3]^-$ presents an interesting contrast (Figure 4e) in that the two PS_2^- moieties are very nearly coaxial, and their dihedral angle is close to 90°, which is consistent with minimization of the repulsion between the two bidentate groups, indicating no distortion resulting from interaction of the TFM groups.

Nucleophilicites from Dissociation of DTP Complexes with Eu^{3+} Nitrate. Dissociation experiments were also performed on mixed ligand complexes that included europium with nitrate anions as well as L_u^- and L_n^- ligands, in order to determine whether the dissociation trends observed in the Na^+ complexes were similar to what would occur in an *f*-element complex. ESI of $Eu(NO_3)_3$ solutions with the dithiophosphinate ligands resulted in production of a series of ions having the general formula $[Eu(anions)_4]^-$, where the anions consisted of combinations of nitrate, L_u^-, and L_n^- (Figure 5).

Initial experiments were focused on competitive dissociation reactions of $[Eu(NO_3)_2(L_u)(L_n)]^-$, which were formed

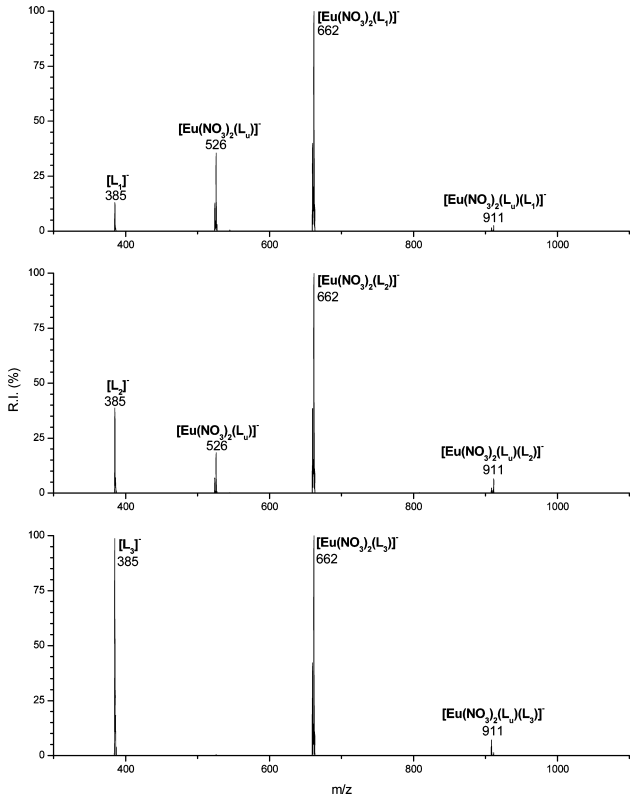

Figure 6. Comparative CID spectra of $[Eu(NO_3)_2(L_u)(L_n)]^-$. Species containing different L_n^- anions are compared: L_1^- (top), L_2^- (middle), and L_3^- (bottom).

in abundance. Collision induced dissociation produced two types of reactions: a redox elimination (RE) of $L_u^\bullet$ and $L_n^\bullet$ (radicals), resulting in reduction of the Eu^{3+} center and ionic dissociation (ID) producing L_n^- and neutral $[Eu(anions)_3]$ (Figure 6, Table 5). Instrumental limitations prohibited observation of nitrate products.

When L_1^- was present in the dinitrato complex $[Eu(NO_3)_2(L_u)(L_1)]^-$, the RE channels accounted for ~90% of the total dissociation products (Table 5, rows 1–3), compared to formation of L_1^- by ID. This changed as L_2^- and L_3^- were substituted for L_1^- in the dinitrato complexes: the fraction of RE dropped to 75% in the L_2^--containing complexes and was only ~11% for L_3^--containing complexes. This overall trend suggests that attachment of two strong donors (i.e., L_u^- and L_1^-) to the Eu^{3+} center increases the tendency of the complex to dissociate via RE pathways. In comparing the ratios of the RE losses of the L_u radical to the L_n radicals, loss of the strongest nucleophile $L_u^\bullet$ as a radical is preferred in all cases compared to loss of any of the L_n radicals. In comparing the RE of $L_n^\bullet$ radicals, $L_1^\bullet$ is eliminated in higher abundance than is $L_2^\bullet$, which in turn is eliminated in higher abundance than is the $L_3^\bullet$. The RE process involves oxidation of the dithiophosphinate ligands by the Eu^{3+} metal center, producing dithiophosphinate radicals: based on the ratios of the dissociation products, it is clear that the tendency of the ligands to undergo oxidation mirrors the relative nucleophilicity, i.e., $L_3^- < L_2^- < L_1^- < L_u^-$.

In contrast to the experiments with the Na^+ complexes, no comparisons of L_n^- nucleophilicity could be made based on the ID processes, because in each case, the parent $[Eu(NO_3)_2(L_u)(L_n)]^-$ fragmented to furnish only L_n^-, and L_u^- was not observed in any of the experiments. As in the case of the sodium complexes, L_u^- is clearly a much stronger nucleophile than are any of the L_n^- anions, to the extent that the data did not enable comparisons of the L_n^- ligand nucleophilicity.

Two different mononitrato complexes were generated as well that had the general formulas $[Eu(NO_3)(L_u)_2(L_n)]^-$ and $[Eu(NO_3)(L_u)(L_n)_2]^-$. For the $[Eu(NO_3)(L_u)_2(L_n)]^-$ complexes, the loss of L_u and loss of L_n as radicals (by RE) was observed, but in these complexes, ionic dissociation is the dominant process. When L_n^- is L_1^-, ionic dissociation results in elimination of neutral $[Eu(NO_3)(L_u)_2]$ (86.7%), with only a trace of $[Eu(NO_3)(L_u)(L_1)]$ (Table 5, rows 4–6). The redox eliminations are less abundant, with loss of $L_u^\bullet$ being favored over loss of $L_1^\bullet$ by a ratio of 11.9:0.7. Consistent with the earlier results L_u^-, being the stronger nucleophile, is preferentially oxidized in the CID process.

In the $[Eu(NO_3)(L_u)_2(L_2)]^-$ complex, the abundance of the RE processes are decreased to only 2.5% and only loss of L_u radical occurs. Instead, ID produces loss of neutral $[Eu(NO_3(L_u)_2]$ forming L_2^- exclusively, i.e., no L_u^- is formed. For the $[Eu(NO_3)(L_u)_2(L_3)]^-$, ID accounted for the sole fragmentation product, eliminating neutral $[Eu(NO_3)(L_u)_2]$ and forming $[L_3]^-$ exclusively. Taken together, these results support the earlier conclusions, viz., that the order of nucleophilicity and ease of oxidation of the ligands both follow the same trend, $L_3^- < L_2^- < L_1^- < L_u^-$.

A second group of mononitrato ligands was studied, having the general composition $[Eu(NO_3)(L_u)(L_n)_2]^-$. The same patterns were observed as in the case of the dinitrato and di-L_u^- complexes, with the exception that, for the $[Eu(NO_3)(L_u)(L_1)_2]^-$ complex, redox elimination of radical L_1 is more prevalent than loss of radical L_u (Table 5, rows 7–9). This difference is partly due to the fact that statistically loss of L_1 is more probable than L_u, and arithmetically accounting for this difference results in the same ordering of the ligands in terms of propensity to undergo oxidation.

Conclusions

Diphenyldithiophosphinate (DTP) ligands substituted with trifluoromethyl at the ortho positions of the phenyl groups have been shown to have superior abilities to effect Am^{3+}/Eu^{3+} separations; however, the details of the physical coordination chemistry responsible have not yet been identified. Differential metal–ligand complex stability has been hypothesized to be responsible for the differences in complex partitioning between the aqueous and organic phase. As part of an ongoing effort to understand the intrinsic chemistry behind the complexation behavior, calculations and experiments were performed that were designed to evaluate the acidity and relative nucleophilicity of the ligands. DFT calculations showed that pK_a values for the free acids decreased $HL_3 < HL_2 < HL_1 < HL_u$, where HL_u is the unmodified DTP, HL_1 is the *bis*(*ortho*-TFM) derivative, and HL_2 and HL_3 are the (*ortho*,*meta*)- and *bis*(*meta*)-versions, respectively. The free acid HL_u was the weakest acid consistent with the e^--donating character of the unmodified

Table 5. Loss Ratios for $[Eu(NO_3)_2(L_u)(L_n)]^-$, $[Eu(NO_3)(L_u)_2)(L_n)]^-$, and $[Eu(NO_3)(L_u)(L_n)_2]^-$

	redox elimination (RE)					ionic dissociation (ID)				
parent ion	loss of neutral L_u	loss of neutral L_1	loss of neutral L_2	loss of neutral L_3	total RE	loss of neutral $Eu(NO_3)_2(L_u)$	loss of neutral $Eu(NO_3)_2(L_n)$	loss of neutral $Eu(NO_3)(L_u)_2$	loss of neutral $Eu(NO_3)(L_u)(L_n)$	total ID
$[Eu(NO_3)_2(L_u)(L_1)]^-$	63.0	26.2			89.2	10.8	>0.7			10.8
$[Eu(NO_3)_2(L_u)(L_2)]^-$	56.9		11.6		68.5	31.4	>0.4			31.4
$[Eu(NO_3)_2(L_u)(L_3)]^-$	41.7			>0.6	41.7	58.1	>0.6	1	1	58.1
$[Eu(NO_3)(L_u)_2(L_1)]^-$	11.9	0.7			12.6			86.7	0.7	87.4
$[Eu(NO_3)(L_u)_2(L_2)]^-$	2.5		>0.4		2.5			97.5	>0.4	97.5
$[Eu(NO_3)(L_u)_2(L_3)]^-$	>0.9			>0.9	0			100.0	>0.9	100.0
$[Eu(NO_3)(L_u)(L_1)_2]^-$	13.3	21.3			34.6				65.4	65.4
$[Eu(NO_3)(L_u)(L_2)_2]^-$	11.1		8.6		19.7				80.3	80.3
$[Eu(NO_3)(L_u)(L_3)_2]^-$	11.7	1	1	>0.5	11.7	1	1	1	88.3	88.3

phenyl groups. Among the TFM derivatives, HL_1 was the weakest, followed (in order) by HL_2 and HL_3. The fact that HL_3 was the strongest acid was surprising since TFM attached at the meta position should be less effective at inductive withdrawal of e^- density, compared to derivatives containing an *ortho*-TFM moiety. Careful analysis of the DFT-generated structures showed that locating the TFM derivatives at the ortho positions of the phenyl rings induced structural alterations, straining the molecule and possibly lessening the effectiveness of inductive e^- withdrawal by the TFM. The structures also posed a second possibility, viz., donation of e^- density to the thiophosphoryl as a result of close proximity of F atom(s) to the phosphorus atom in the lowest energy conformations.

Ligand nucleophilicities were evaluated by forming mixed ligand–metal complexes in the gas phase, which were then activated and dissociated. Competitive fragmentation of $[Na(L_u)(L_{n=1,2,3})]^-$ complexes showed that in all cases the unmodified diphenyldithiophosphinate ligand L_u^- was the strongest nucleophile relative to Na^+. Among the TFM derivatives, the relative nucleophilicities followed the trend $L_3^- < L_2^- < L_1^-$, following the same order observed for the pK_a values. As in the case of the pK_a trend, the trend in nucleophilicities is counterintuitive based on inductive effects expected for the *ortho*- and *meta*-TFM derivatives. DFT calculations of the *ortho*-TFM derivatives complexed with Na^+ showed that the lowest energy rotational conformations involved significant interactions between the metal and two F atoms. This is a different explanation from those likely responsible for the trend in pK_a values and hints that multiple factors may be responsible for the selective complexation observed in the *f*-element separations experiments.

Dissociation experiments of mixed-ligand europium complexes such as $[Eu(NO_3)_2(L_u)(L_n)]^-$ fragmented by ionic dissociation but these produced only the TFM-modified diphenyldithiophosphinate ligands $[L_{n=1,2,3}]^-$, showing that the unmodified diphenyldithiophosphinate L_u^- was the stronger nucleophile in all cases but did not enable further comparisons regarding the nucleophilicity of the L_n^- ligands. On the other hand, the complexes also underwent redox elimination reactions, in which the strong nucleophilic ligands underwent oxidation and were eliminated as radicals. The unmodified diphenyldithiophosphinate was most extensively oxidized, followed by complexes containing an *ortho*-TFM derivative. Thus, the trend for susceptibility to oxidation was the same as that for nucleophilicity and DFT-calculated pK_a values, i.e., $L_3^- < L_2^- < L_1^- < L_u^-$.

Acknowledgment. Work by G.S.G., G.L.G., M.T.B., J.K., M.M., and D.P. was supported by the U.S. Department of Energy, INL Laboratory Directed Research & Development Program under DOE Idaho Operations Office Contract DE-AC07-05ID14517. M.J.V.S. was supported under INL Education Programs Faculty Staff Exchange and C.M.L. was supported by the U.S. Department of Energy, Office of Science, Science Undergraduate Laboratory Internships program. J.-J.G. and F.A. were supported by the University of Metz and the Ministere de l'Education Nationale, de la Recherche et de la Technologie (France).

Supporting Information Available: Selected bond lengths, Mulliken atomic charges, and cartesian coordinates. This materials is available free of charge via the Internet at http://pubs.acs.org.

IC7020897